CF-2949

T H E U N I V E R S I T Y O F M I C H I G A N
COLLEGE OF ENGINEERING
Department of Aeronautical and Astronautical Engineering

Technical Report

EXPERIMENTAL INVESTIGATION OF JET-SIMULATED FLARE STABILITY OF AN OGIVE-CYLINDER AT SUPERSONIC SPEEDS

Gerard F. Carvalho

ORA Project 03942

under contract with:

DEPARTMENT OF THE NAVY
BUREAU OF NAVAL WEAPONS
CONTRACT NO. NOrd-16595
WASHINGTON, D.C.

through:

APPLIED PHYSICS LABORATORY
THE JOHNS HOPKINS UNIVERSITY
SILVER SPRING, MARYLAND

administered through:

OFFICE OF RESEARCH ADMINISTRATION ANN ARBOR

January, 1962

ABSTRACT

An investigation, conducted to determine the feasibility of simulating a body flare by means of jets exhausting around the circumference of the body in close proximity to the base, has revealed that the stability of non-lifting bodies of revolution can be increased by use of jet-simulated flares.

TABLE OF CONTENTS

LIST OF FIGURES

LIST OF SYMBOLS

A_b base area.

C_M pitching moment coefficient = $\frac{\bar{N}x}{q_\infty A_b L}$

ΔC_M change in pitching moment coefficient = C_M jet on - C_M jet off.

C_N normal force coefficient = $\frac{N}{q_\infty A_b}$

ΔC_N change in normal force coefficient = C_N jet on - C_N jet off.

C_p pressure coefficient = $\frac{p - p_\infty}{q_\infty}$.

D body base diameter.

d throat diameter of nozzle.

$\frac{dC_M}{d\alpha}$ rate of change of pitching moment coefficient with angle of attack.

$\frac{dC_N}{d\alpha}$ rate of change of normal force coefficient with angle of attack.

$\frac{dC_p}{d\,x/L}$ rate of change of pressure coefficient with distance along ogive-cylinder axis.

f fineness ratio of ogive-cylinder.

f_n fineness of ratio of ogive.

L body length.

$\dot{M}$ mass flow parameter = $\frac{\dot{m}}{\rho_\infty V_\infty A_b}$.

M_∞ free-stream Mach number.

M_j jet exit Mach number.

$\dot{m}$ measured mass flow.

N normal force.

p static pressure on body.

q_∞ free-stream dynamic pressure.

Re Reynolds number, based on body length.

LIST OF SYMBOLS (Concluded)

V_∞	free-stream velocity.
x	longitudinal distance from vertex.
$\bar{x}$	center of pressure location ahead of center of gravity.
α	angle of attack.
ρ_∞	free-stream density.

INTRODUCTION

Aerodynamic vehicles which can be described as non-lifting bodies of revolution, with either pointed or blunt nose shapes and cylindrical afterbodies, are generally statically unstable about their centers of volume. Static instability may be desirable for some of these vehicles, while for others this condition may be intolerable. If a vehicle of the type discussed must have a degree of static stability not offered by its aerodynamic characteristics, the designer is faced with the problem of determining what device or devices will best provide the static stability desired.

The static stability of a given aerodynamic vehicle can be increased (or decreased) by means of auxiliary lifting surfaces, body flares, flow separation on the body caused by interaction of the expanding propulsive jet and the free stream, and also by simulating a body flare with side jets located around the circumference of the body. This report contains the results of an investigation of the ability of side jets to increase the stability, about the center of volume, of an ogive-cylinder in a supersonic air stream.

A jet exhausting normal to the cylindrical afterbody of an ogive-cylinder traveling at supersonic speeds acts as a blunt body and becomes enveloped in a strong shock wave. This strong shock wave interacts with the boundary layer on the body and

generally causes the boundary layer to separate upstream, laterally, and downstream from the jet. In the investigation reported herein, configurations were tested on which jets exhausted normal to the body all around the circumference of the body near the base. Thus the strong shock waves ahead of each jet coalesced and forced the boundary layer on the body to separate around the entire circumference. The jet flare thus simulated a body flare and a favorable change in stability was obtained.

EXPERIMENTAL EQUIPMENT

Wind Tunnel.-The tests were conducted in the University of Michigan 8-by 13-inch blowdown wind tunnel. The tunnel was operated at atmospheric stagnation pressure and a Mach number of $M_\infty = 3.97$. A description of the wind tunnel and associated equipment, and recent calibration data are contained in References 1 and 2.

Models.-The basic model used in these tests was a fineness ratio of 6.58 ogive-cylinder. The model length was 13.0 inches and the ogive had a radius of 18.5 inches, the proper value for a fineness ratio 3.0 tangent ogive with a diameter of 2.0 inches. However, the diameter of the cylinder had been turned down to 1.975 inches for a previous test program, and the shoulder between the ogive and the cylinder was then rounded to provide a relatively continuous expansion at the shoulder. The resulting modified ogive nose had a fineness ratio of about 2.66.

The model was segmented so that the various jet flare patterns were obtained simply by the installation of spacers with the desired nozzles. Three spacers were constructed, one with 24 sonic nozzles evenly spaced around the circumference (designated in this report as 24-J), one with 12 sonic nozzles evenly spaced around the circumference (designated 12-J), and one with a supersonic slot (designated slot). The nozzle diameter for spacer 24-J was d = 0.119", for 12-J it was d = 0.160", and the

supersonic slot had a 10.5 degree semi-divergence angle with an exit Mach number of $M_j = 3.2$. All nozzles in each of the spacers had smooth contraction sections.

The jet fluid for all models was dry air which was obtained from a high pressure laboratory source and throttled to the desired pressure. Mass flow to the jets was measured by means of a standard ASME sharp-edged orifice. The air was piped from the external supply system to the inside of the model thru the hollow cantilever sting balance upon which the model was mounted.

Tests.-The data obtained during these tests include the forces and moments on the model which was mounted on a hollow cantilever sting balance. Moments applied to the sting balance by the model were measured at four stations along the sting by means of strain gage bridges. Commercial carrier amplifiers with a recording oscillograph comprised the system by which the moments on the sting balance were sensed and recorded. Additional data were obtained by means of schlieren photographs, china clay patterns of the separation line, and pressure measurements in the wake.

The construction of the models was such that the air from the external stream could blow thru the interior of the models when the models were at an angle of attack. Thus, to eliminate the possibility of recording any extraneous forces due to this unwanted circulation of air from the free stream, the jets were turned on before the main tunnel flow was started and turned off after the main tunnel flow had ceased. The angle of attack

range covered for the tests was approximately from $\alpha = -1.00^{\circ}$ to $\alpha = 2.00^{\circ}$

Discussion of Errors.-The strain gage bridges were grouped in pairs - two near the center of the model and two near the base. Thus each force datum point was obtained as the average of four values from the four different combinations of a forward moment and a rearward moment.

Difficulty was encountered in obtaining and reducing the data because the jet gas that passed thru the sting balance forced the sting to vibrate. Considerable vibration was encountered at the higher mass flows and the resultant traces recorded were difficult to interpret. An estimate of the accuracy with which the moments on the sting balance could be determined, and the accuracy of jet mass flow, tunnel pressure and Mach number, and angle of attack was made. It was then determined that, at the higher mass flows, the maximum possible errors in the data presented are:

Model	C_N % C_N max., no jet	C_M % C_M max., no jet	Separation Line Location % L
24-J	± 5.0	± 9.0	± 1/2
12-J	± 4.0	± 9.0	± 1/2
Slot	± 9.0	± 9.0	± 1/2

DISCUSSION OF TEST RESULTS

The ogive-cylinder characteristics and the separation line variation with mass flow parameter for the three models tested are contained in Fig. 1. The pressure gradient in Fig. 1(b) was obtained by measuring the slope of the pressure profile as calculated by the second-order shock-expansion method.[3]

The third section of the first figure, Fig. 1(c), shows the location of the separation line at $\alpha = 0^{o}$ for each of the models tested. Configurations 24-J and 12-J, both of which had the jets located at $\frac{x}{L} = 0.913$, do not have equal separation distances for equivalent values of the mass flow parameter. Configuration 12-J, it must be remembered, had more total space between the nozzles than did 24-J. Thus it is surmised that 12-J was incapable of containing as large a pressure build-up in the separation zone as 24-J, with the result, as indicated in Fig. 1(c), that the separation zone is not as extensive in the upstream direction. The center line of the jet for the slot model was located at $\frac{x}{L} = 0.962$. As mentioned previously, the construction of the slot was such that the supersonic jet allowed no passage for the high pressure air in the separation zone to travel along the body from the separation zone to the base region of the body. This test configuration, for small values of the mass flow parameter, forced the boundary layer separation point to stabilize farther upstream from the jet center line than either 24-J or

12-J. A similiar result was noted earlier[4], when the area thru which high pressures in the separation zone created by a single sonic jet could travel to the base was reduced by means of fins.

The changes in the longitudinal stability parameters caused by the jet-simulated flare are plotted in Fig. 2. All three models tested produced favorable changes in the stability of the ogive-cylinder, with model 12-J providing the greatest improvement in stability. The curves of pitching moment variation with angle of attack were linear throughout the angle of attack range of the tests and the curves of normal force variation with angle of attack tended to become linear as the mass flow parameter increased.

It is interesting to discuss the variations of the pitching moment curve slope with mass flow parameter as plotted in Fig. 2(b), when Fig. 1(c) is kept clearly in mind. The curves of Fig. 2(b) show an initial sharp increase in stability with mass flow for model 12-J and less pronounced increases for the other test configuration. This increase in stability continues up to a value of $M \approx .15$ for both 12-J and 24-J and up to a value of $M \approx .1$ for the slot. Considering now Fig. 1, it is seen that this increase in stability roughly corresponds to the case for which separation occurs on the cylindrical part of the body for all configurations.

Then for models 12-J and 24-J, there is a decrease in stability as the mass-flow parameter varies from approximately 0.15 to 0.45. Again refering to Fig. 1 it is seen that within

this range of $\dot{M}$, the separation line is quite close to the actual shoulder of the test model, that is, in this range of mass-flow parameter for 12-J and 24-J, the separation line is pushed over the shoulder and into the region of favorable pressure gradient on the ogive. The third section of the curves, of pitching moment slope variation for 12-J and 24-J, i.e. $\dot{M}>0.45$, show, once again, an increase in stability. For this range of mass flow, it is seen, by referring to Fig. 1, that the separation point is well ahead of the body shoulder and into the region of favorable pressure gradient on the ogive.

The slot model does not exhibit all the characteristics of 12-J and 24-J as is easily seen in Fig. 2(b). For small values of the mass flow parameter, the stability of the slot model increases at a moderate rate followed by a more gradual increase in stability, without the decrease as noted for 12-J and 24-J. Scrutiny of Fig. 1 reveals that for the range of mass-flows tested for the slot, the separation line remains in the vicinity of the shoulder. No explanation is presented at this time for the differences in behavior between the different models when the separation line is in the vicinity of the shoulder.

The data presented in Fig. 2 were obtained by measuring the slopes of the curves of normal force coefficient and pitching moment coefficient versus angle of attack, such as the curves contained in Figs. 3 and 4. The curves of C_N vs α and C_M vs α were linear within the angle of attack range of the test pro-

gram for all values of the mass flow parameter. The curves of Figs. 3 and 4 were obtained by cross-plotting from curves of C_N and C_M versus mass flow parameter, $\dot{M}$ for the various angles of attack at which measurements were made. The curves of C_N versus $\dot{M}$ and C_M versus $\dot{M}$ were faired thru the measured values of C_N and C_M so that the scatter in C_N and C_M is displayed in Figs. 3 and 4. The shifting of the curves of C_N versus α and C_M versus α, in Figs. 3 and 4, for the body with the jet-simulated flare, is believed due to a slight asymmetry which resulted from slight differences in the dimensions between individual sonic nozzles of 24-J and 12-J and due to slight differences in throat thickness around the circumference of the slot.

Plotted in Fig. 5 is the change in normal force coefficient at one degree angle of attack due to the jet flare for the three models tested and also data for a blunt-cone cylinder model.[5,6] Also included in Fig. 5 are data[4] for a single side jet on an ogive-cylinder identical to the one used in the present tests, and the values of the normal force coefficient at $\alpha = 1^{o}$ for the ogive-cylinder of these tests and the blunt cone-cylinder.

The restoring moments provided by each of the configurations tested are plotted in Fig. 6. For 12-J and 24-J, the curves are extrapolated linearly to the point where neutral stability will perhaps be obtained with the jet-simulated flares. If the curves of Fig. 1(c), indicating separation line location, are extrapolated up to the values of mass flow necessary for neutral stability

then it is seen that the separation points for 12-J and 24-J lie on the ogive in the region where the pressure gradient does not change rapidly. In fact, the change in pressure gradient is almost constant from the shoulder to the neutral stability separation point as estimated by means of these various extrapolations.

The slot is seen to be, in general, the least efficient of the three configurations tested. This may be due, in part, to the fact that the slot model jet was located closer to the base than the jets of the other models. It is approximately true, except for those values of M for which the separation point is in the immediate vicinity of the shoulder, that moving the jets closer to the base of the body reduced efficiency as can be inferred from Figs. 1 and 2.

The tests using a blunt cone-cylinder model[5], in which nitrogen was used as the jet fluid, were conducted to determine the stabilizing influence of the main rocket exhaust. Some of the results obtained are included in Fig. 6 because the jet configuration tested is a limiting case. The jet is located at the base of the body, and the jet thrust vector is parallel to the body axis. Also, similar to the slot used in this investigation, the jet completely enveloped the circumference of the model so that the high pressures within the separated zone could not escape downstream thru the jet.

A jet-simulated flare is not the same type of device as a single side jet, but when one thinks in terms of ability of a device to return a vehicle to its prescribed flight path, then

it is useful to compare the efficiencies of the various devices which can perform this feat. For this reason, there is included in Fig. 6, for comparison purposes, the restoring moment imparted to the ogive-cylinder by a single side jet. Data available[7] indicate that the change in total normal force produced by a single side jet with angle of attack is negligible for small angles. It is assumed, therefore, that the data obtained at zero degree angle of attack[4], can be plotted on Fig. 6 without introducing excessive error.

Schlieren photographs of 24-J and the slot are contained in Fig. 7. Light and dark areas on the model can be discerned in some of the photographs. The dark areas correspond to regions of heavy concentration of china-clay on the model while the light areas correspond to regions on the model where the china-clay is either completely absent or present in a very light film.

The designer is interested not only in the amount of stability that can be obtained by employment of a particular device, but also the change in drag induced by the device. No drag measurements were made during this investigation, but a limited number of pressure measurements were made in the wake of the body. The configuration 12-J provided the least relative increase in pressure drag and the slot configuration provided the greatest relative increase in pressure drag.

CONCLUSIONS

Analysis of the data obtained during the investigation reported herein provides the basis for the following conclusions:

1. Stability of a non-lifting body of revolution can be favorably influenced by a jet-simulated body flare.

2. Some of the more important parameters governing the problem are pressure gradient on the body, type (sonic or supersonic) of nozzles used, location of nozzles relative to the base of the body, spacing between the nozzles, and inclination of the nozzles to the body axis.

REFERENCES

1. Garby, L.C., and Nelson, W.C., University of Michigan 8 x 13-inch Intermittent-Flow Supersonic Wind Tunnel, UMM-59, University of Michigan Engineering Research Institute, June, 1950.

2. Carvalho, G.F., Calibration Report on the University of Michigan 8-by 13-inch Supersonic Wind Tunnel, Calibration at Nominal Mach Number of 3.90, WTM-268, The University of Michigan Research Institute, March, 1960.

3. Syvertson, C.A., and Dennis, D.H., A Second-Order Shock Expansion Method Applicable to Bodies of Revolution Near Zero Lift, NACA Report 1328, 1958.

4. Carvalho, G.F., and Hays, P.B., Jet Interference Experiments Employing Body-Alone and Body-Fin Configurations at Supersonic Speeds, 03942-7-T, CM-979, The University of Michigan Research Institute, December, 1960.

5. Salmi, R.J., Effects of Jet Billowing on Stability of Missile Type Bodies at Mach 3.85, NASA TN-D-284, June, 1960.

6. Private communication with R.J. Salmi, June, 1961.

7. Vinson, P.W., and Amick, J.L., and Liepman, H.P., Interaction Effects Produced by Jet Exhausting Laterally Near Base of Ogive-Cylinder Model in Supersonic Main Stream, NASA Memo 12-5-58W, February, 1959.

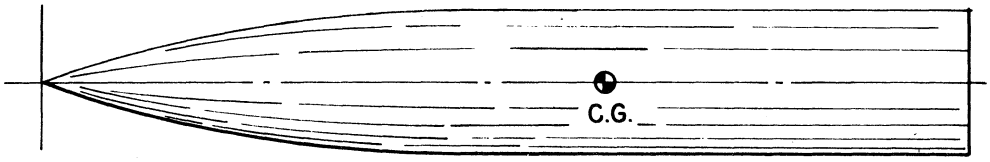

(a) OGIVE - CYLINDER

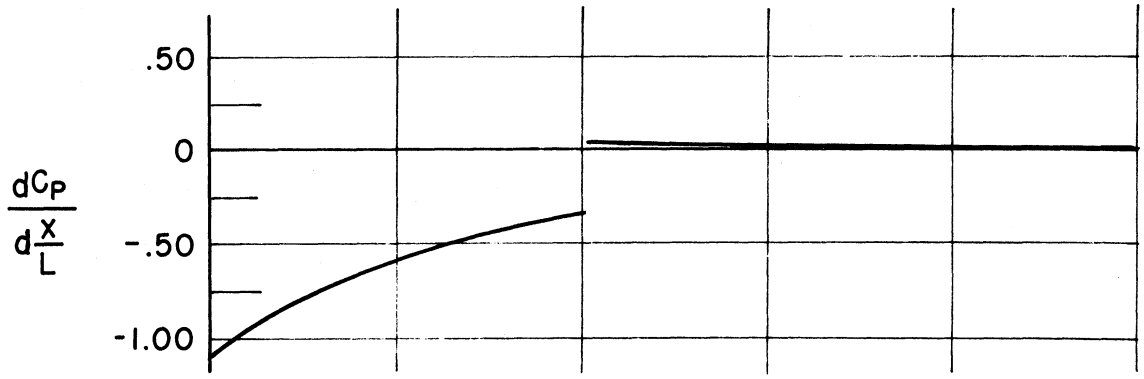

(b) THEORETICAL PRESSURE GRADIENT ON OGIVE - CYLINDER

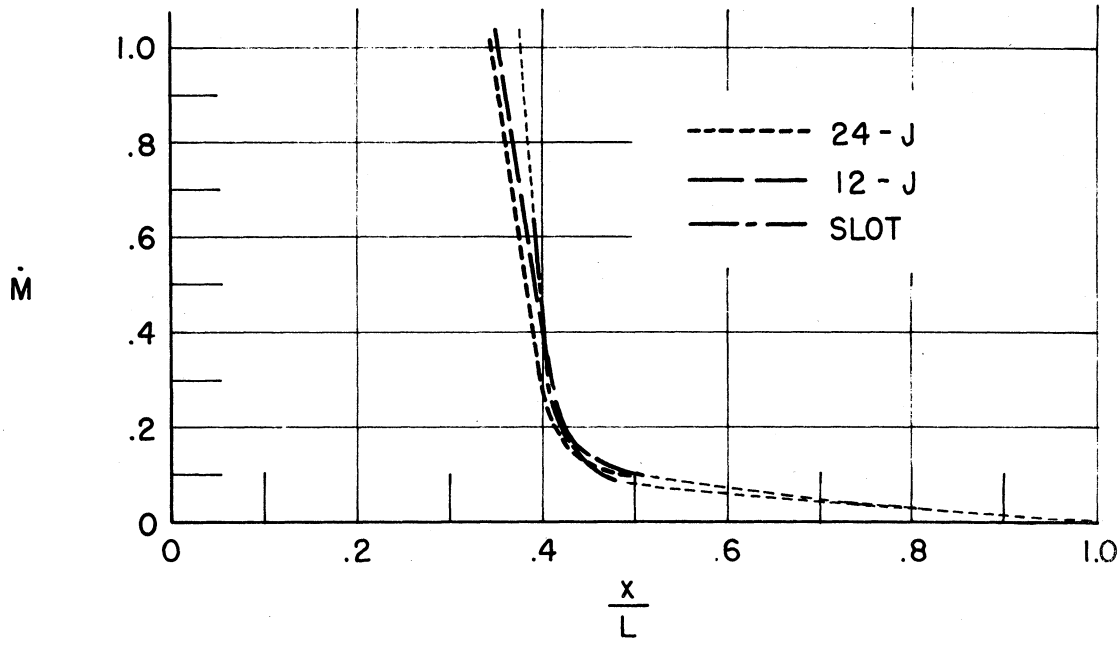

(c) SEPARATION LINE LOCATION AT $\alpha = 0°$

FIGURE 1. OGIVE - CYLINDER CHARACTERISTICS AND SEPARATION LINE VARIATION . $M_\infty = 3.97$, $Re = 1.63 \cdot 10^6$, $f = 6.58$, $f_n = 2.66$, LAMINAR BOUNDARY LAYER .

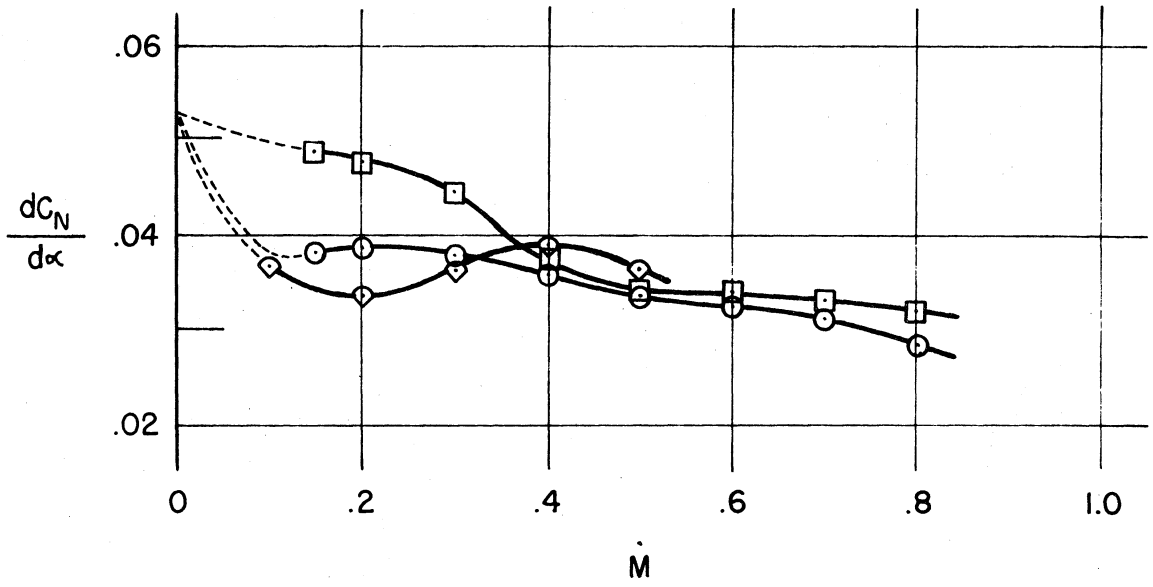

(a) NORMAL FORCE CURVE SLOPE VARIATION WITH MASS FLOW PARAMETER

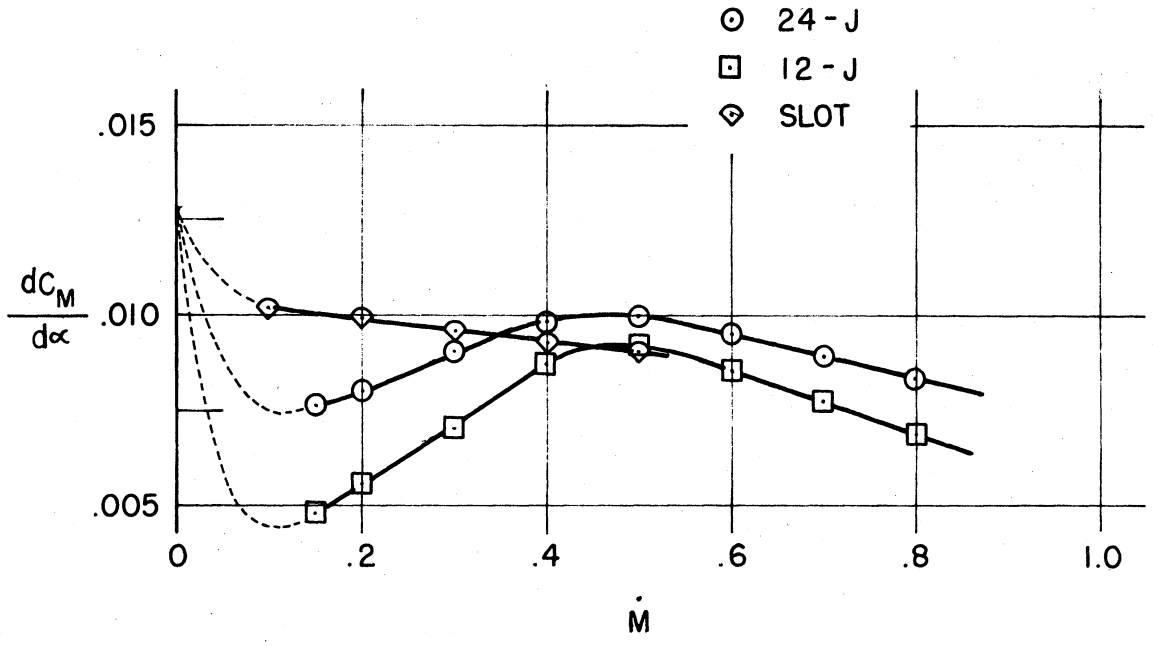

(b) PITCHING MOMENT CURVE SLOPE VARIATION WITH MASS FLOW PARAMETER

FIGURE 2. EFFECT OF JET - SIMULATED FLARE ON LONGITUDINAL STABILITY PARAMETERS OF AN OGIVE - CYLINDER. $M_\infty = 3.97$, $Re = 1.63 \cdot 10^6$, $f = 6.58$, $f_n = 2.66$, LAMINAR BOUNDARY LAYER.

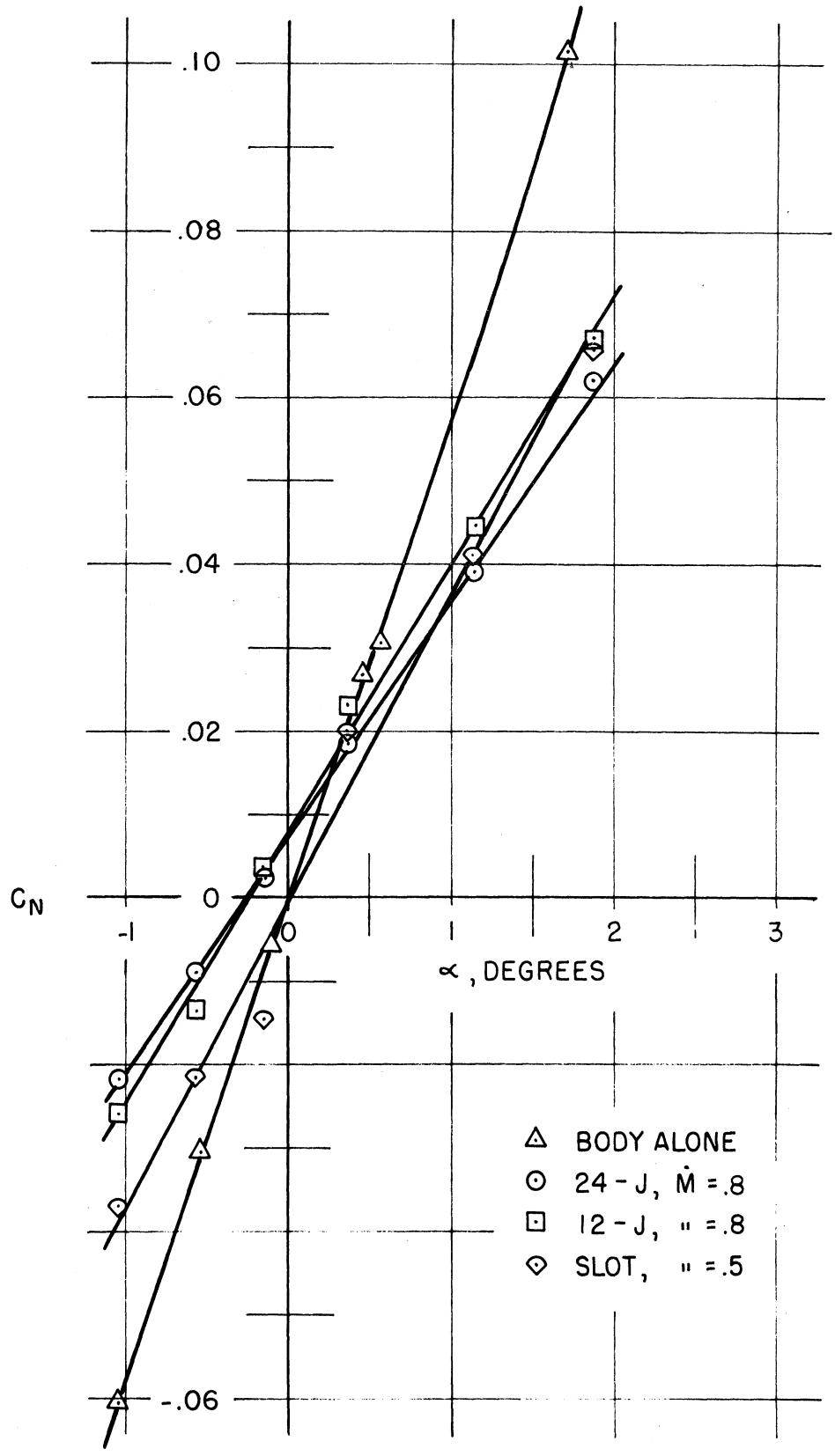

FIGURE 3. NORMAL FORCE COEFFICIENT FOR OGIVE - CYLINDER WITH VARIOUS JET - SIMULATED FLARE CONFIGURATIONS. M_∞=3.97, $Re = 1.63 \cdot 10^6$, f = 6.58, f_n = 2.66, LAMINAR BOUNDARY LAYER.

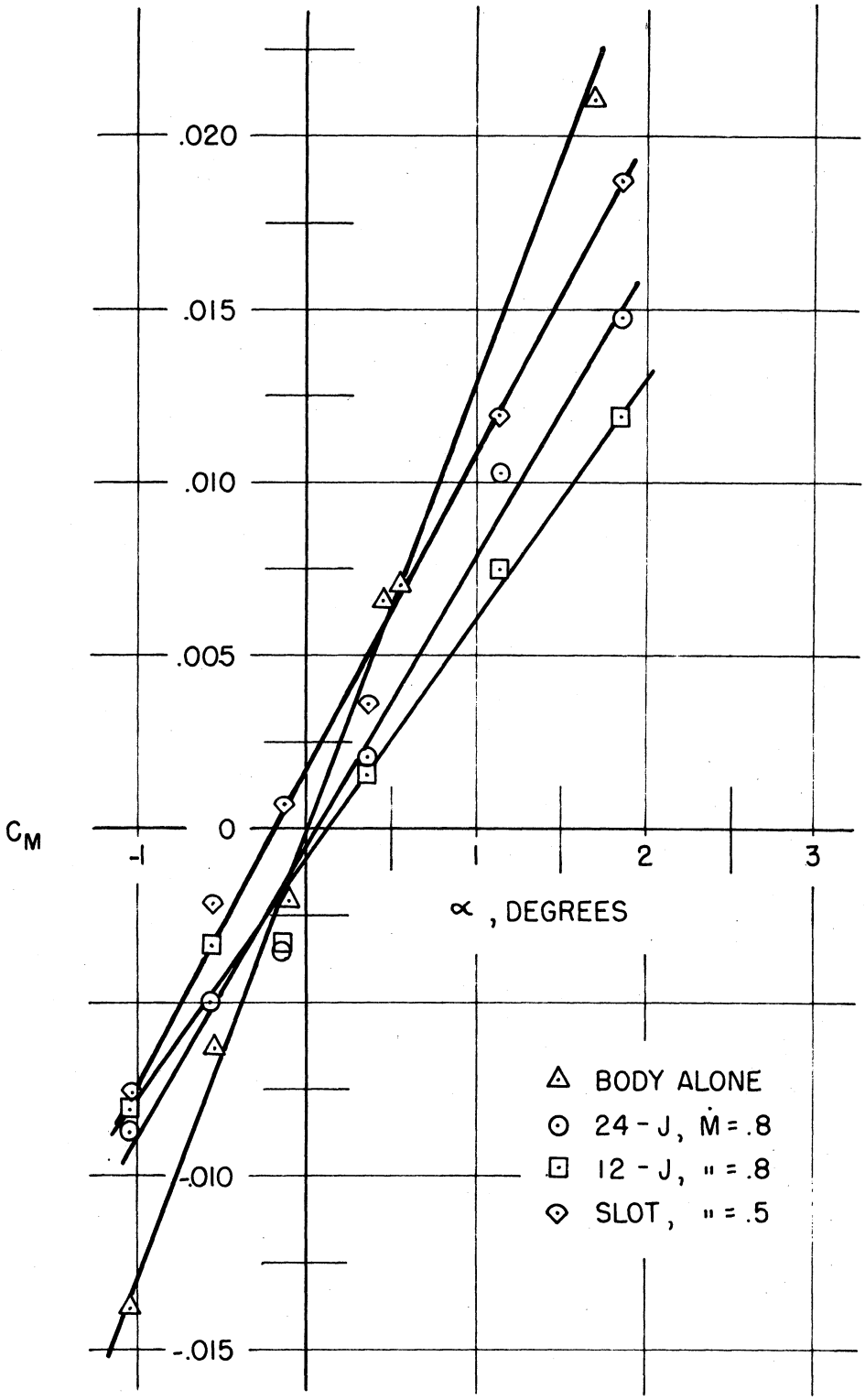

FIGURE 4. PITCHING MOMENT COEFFICIENT FOR OGIVE - CYLINDER WITH VARIOUS JET - SIMULATED FLARE CONFIGURATIONS. $M_\infty = 3.97$, $Re = 1.63 \cdot 10^6$, $f = 6.58$, $f_n = 2.66$, LAMINAR BOUNDARY LAYER .

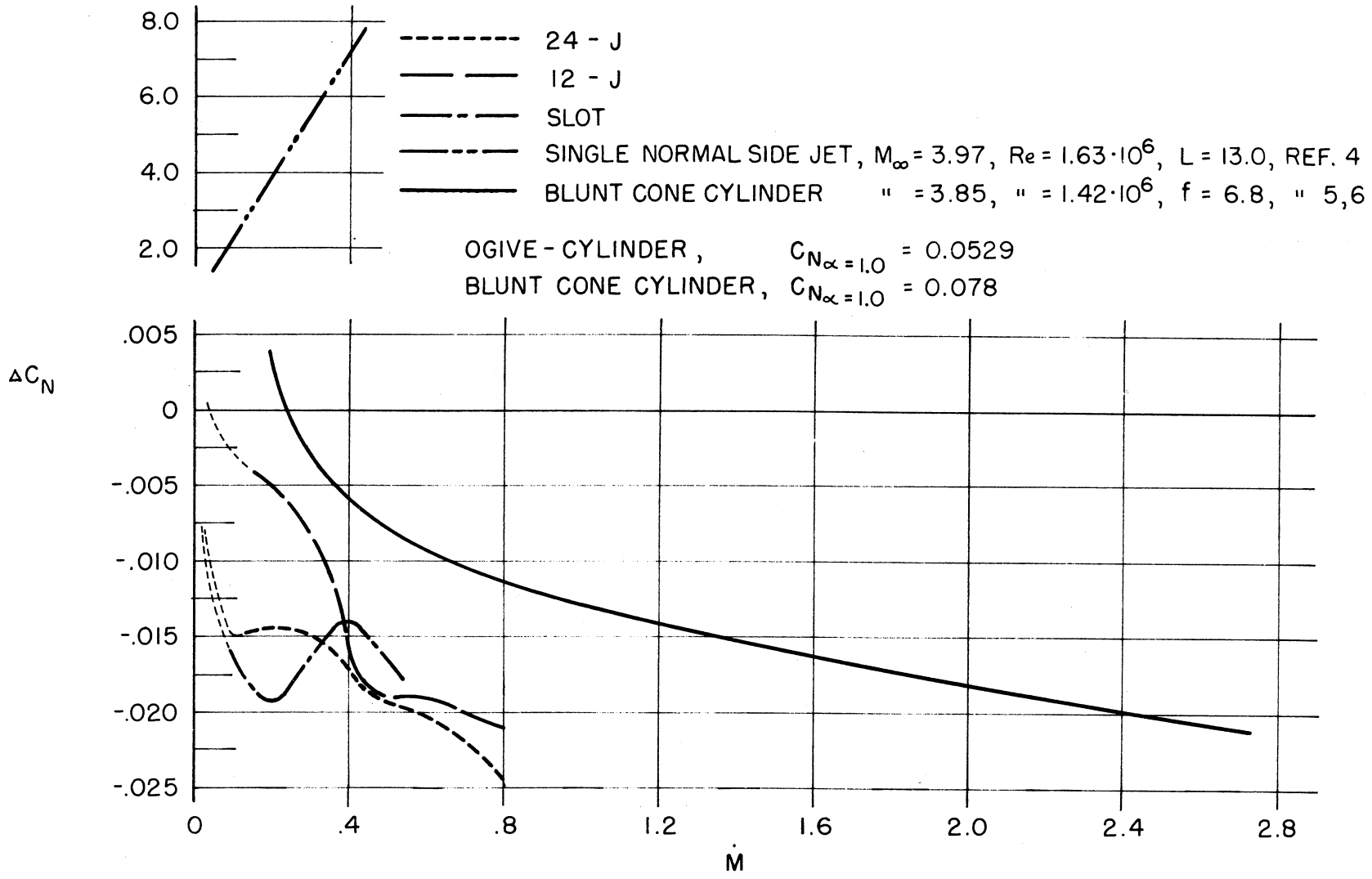

FIGURE 5. CHANGE IN NORMAL FORCE COEFFICIENT AT $\alpha = 1°.0$ FOR OGIVE - CYLINDER WITH VARIOUS JET - SIMULATED FLARES AND A SINGLE SIDE JET CONTROL DEVICE.

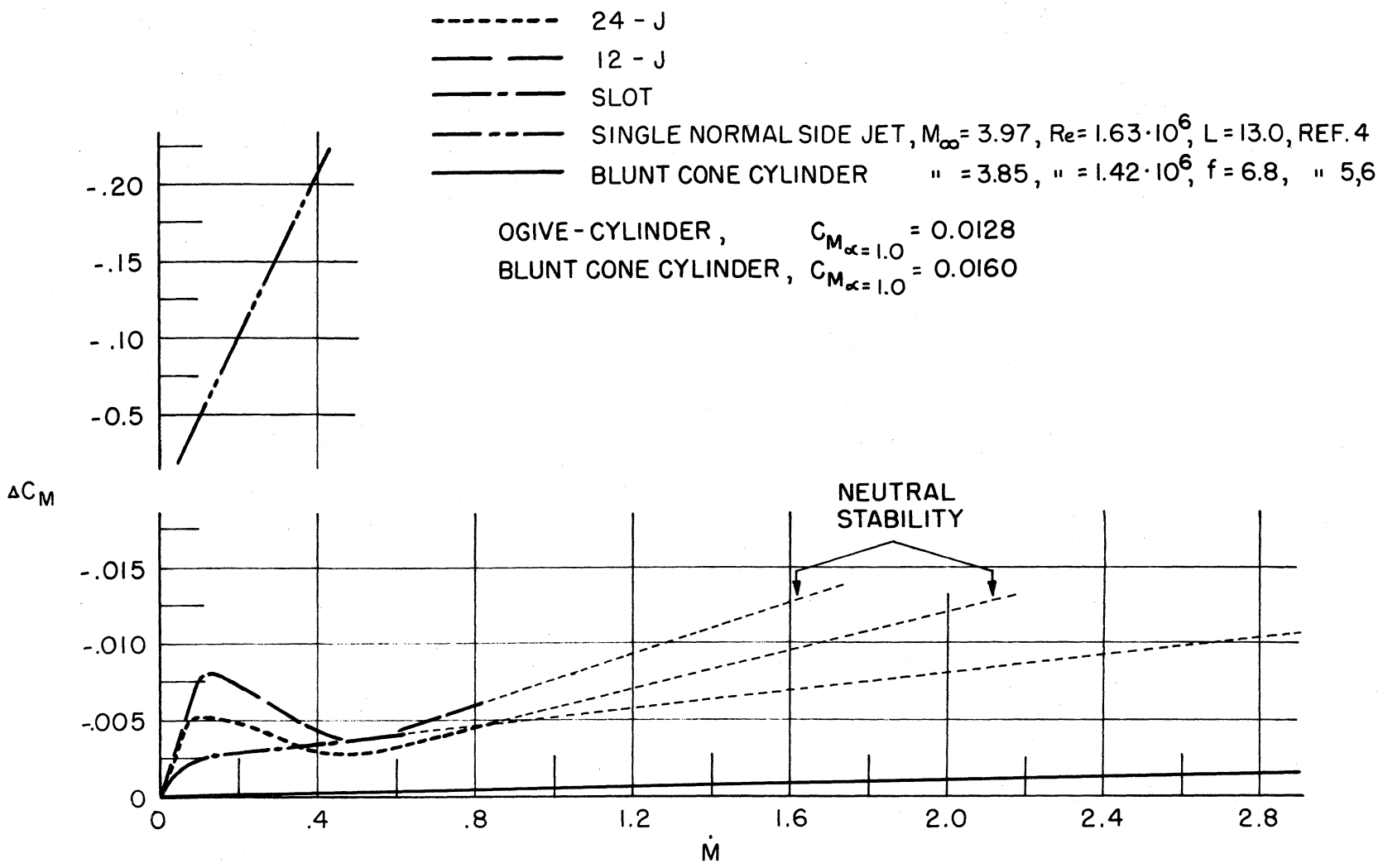

FIGURE 6. RESTORING MOMENT AT $\alpha = 1.0$ FOR OGIVE - CYLINDER WITH VARIOUS JET - SIMULATED FLARES AND A SINGLE SIDE JET CONTROL DEVICE.

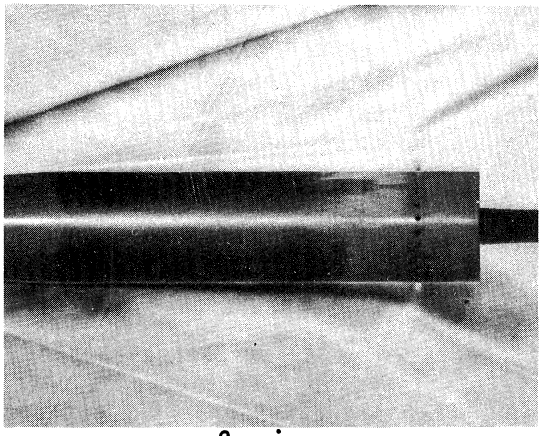

$\alpha = 0°$, $\dot{M} \sim .27$

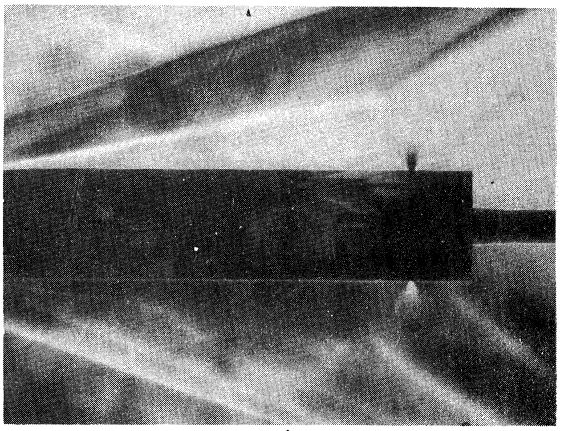

$\alpha = 0°$, $\dot{M} \sim 1.2$

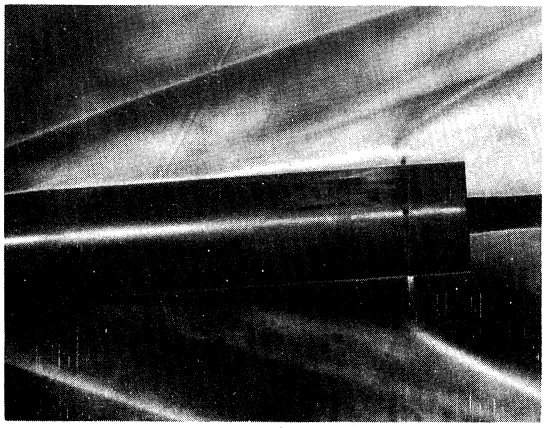

$\alpha = 4°$, $\dot{M} \sim .33$

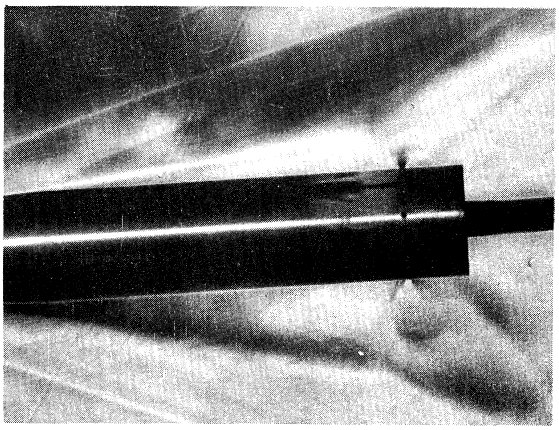

$\alpha = 4°$, $\dot{M} \sim 1.2$

(a) BODY FLARE SIMULATED BY SONIC JETS, 24 - J

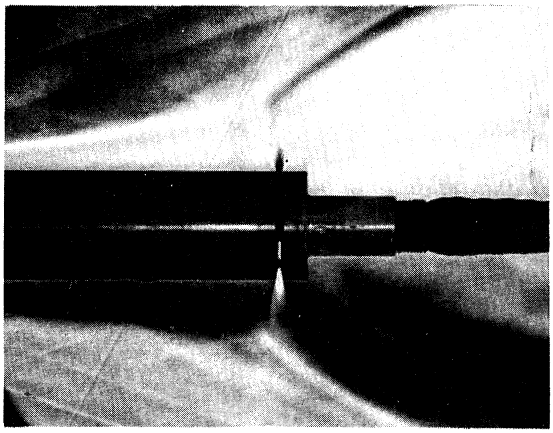

$\alpha = 0°$, $\dot{M} \sim .69$

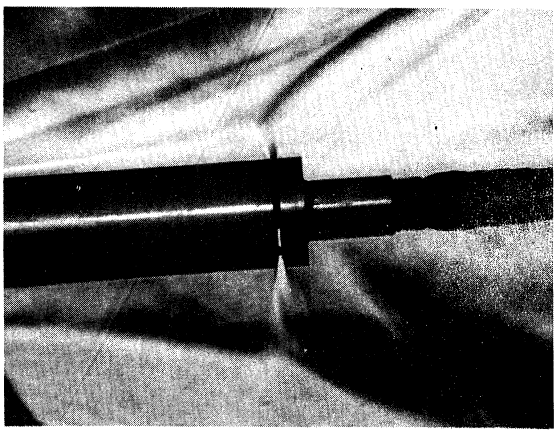

$\alpha = 4°$, $\dot{M} \sim .71$

(b) BODY FLARE SIMULATED BY CIRCUMFERENTIAL SUPERSONIC JET

FIGURE 7. AERODYNAMIC INTERFERENCE PATTERNS PRODUCED BY SIMULATED BODY FLARES. $M_\infty = 3.97$, $Re = 1.63 \cdot 10^6$, OGIVE-CYLINDER, $f = 6.58$, $f_n = 2.66$.